Complementary section

I. INTRODUCTION

Our current understanding of our Universe on large scales is very limited to our observations and surveys for which we try to make sense using our elaborate and ever-developing theories of nature. Einstein's wonderful theory of general relativity provides a framework upon which we can understand some of the phenomena that we see in our data but it still doesn't give us a satisfactory explanation of a very big problem in modern cosmology which is the accelerated expansion of the Universe.

Many explanations have been proposed for this puzzling behaviour of the Universe, as we summarize in section 2, some of them as deviations from Einstein's GR or modifications of it. For obvious reasons those models cannot be directly tested on large scales so we need to rely on the data and the phenomenology of the large scale observations at hand to test them or at least elaborate on their validity.

One interesting way to address this issue is by trying to find a link between the observed phenomenology with a general theoretical approach that allows for the inclusion of all models of cosmic expansion. Many efforts have been put on searching for a unifying approach that could allow for model independent way to study this phenomenology. This work is based on the study of some functions that come naturally from this general theoretical approach but that we can relate to observables and that we call phenomenological functions namely μ and Σ.

In other words, finding ways to understand as much as we can from these functions which have the power of providing insight into the nature of gravity through the phenomenology of large scales [1]. The following section gives a brief introduction to the main question that motivates the quest for finding general models of gravity, which is the problem of the accelerated expansion of the Universe.

II. COSMIC ACCELERATION

In order to understand how the Universe expands we must introduce some background information that will lead naturally to the mathematical expressions of cosmic acceleration.

There are a couple of basic assumptions that we must start from. One has to do with the mathematical form of space time. In the GR framework, we need to solve Einstein equations for the metric $g_{\mu\nu}$ which is the fundamental entity that defines the structure of spacetime. One of the most important constraints on this metric tensor is the homogeneity of the large scale universe (galaxy surveys have supported this claim), that is, on large scales the average density of the Universe is uniform.

The Universe appears to be homogeneous and isotropic so but since the observable Universe does not correspond to all events of the Universe spacetime then we assume the Universe is homogeneous and isotropic as a whole. These assumptions are needed for what follows. In 1921 Hubble had the first reliable observation of galaxies receding from us with speeds that are proportional to their distances. The model of the big bang was to emerge.

Hubble proposed an expression that relates the distance to objects in the sky to their velocity by a constant after his name. This expression is called Hubble's law $v = Hd$ so obtaining the fundamental form of H will result in the relative rate of expansion at a given time. Let's consider the proper distance d from our galaxy to a galaxy with fixed comoving coordinate χ at a given time t. This proper distance is given by:

$$d(t) = a(t)\chi \tag{1}$$

Where the functional form of the comoving distance χ is given by

$$\chi(r) = \begin{cases} \sin^{-1} r & \text{if} \quad k = 1 \\ r & \text{if} \quad k = 0 \\ \sinh^{-1} r & \text{if} \quad k = -1 \end{cases} \tag{2}$$

and depends on the curvature of spacetime. Deriving the last expression w.r.t time we find that the change in proper distance as time passes is

$$v = \frac{\dot{a}(t)}{a(t)} d(t) \tag{3}$$

So comparing this with Hubble's law we have proved that the expansion rate of the universe H at a given time t is given by

$$H(t) = \frac{\dot{a}(t)}{a(t)} \tag{4}$$

At present time t_0, the expansion is (above equation) evaluated at t_0 which is called the Hubble constant and denoted by H_0. It is useful to parametrize Hubble's constant as

$$H_0 = h \frac{100 \text{ km}}{\text{s Mpc}} \tag{5}$$

So that when we determine parameter h, we determine Hubble's constant (today $h \approx 0.7$ so $H_0 \approx 70$ km/s/Mpc). If the galaxy is in our neighbourhood it is trivial to prove that the velocity in eq. (3) is equal to the redshift z. To prove this consider a galaxy near to us. In terms of cosmic time it means that the time passed between photon emission t_1 and observation t_0 is given by a very small quantity Δt; it also means that the cosmic recession velocity is very small, or $v \ll 1$. Using the expression that relates the redshift with the scale size of the Universe $1 + z = a(t_0)/a(t)$ we get

$$1 + z = \frac{a(t_0)}{a(t_0 - \Delta t)} \approx \frac{a(t_0)}{a(t_0) - \dot{a}(t_0)\Delta t} \tag{6}$$

which for $\Delta(t)$ very small we can approximate to

$$1 + z \approx 1 + \frac{\dot{a}(t_0)}{a(t_0)\Delta t} \tag{7}$$

Now consider t_1 as the time of emission, i.e., $t_1 = t_0 - \Delta t$. For a small Δt we have

$$\int_{t_1}^{t_0} \frac{dt}{a(t)} = \int_{t_1}^{t_1 + \Delta t} \frac{dt}{a(t)} \approx \frac{\Delta t}{a(t_1)} \approx \frac{\Delta t}{a(t_0)} \tag{8}$$

On the other side, since we are following a photon's geodesic we get

$$\int_{t_1}^{t_0} \frac{dt}{a(t)} = -\int_{r_1}^{0} \frac{dr}{\sqrt{1-kr^2}} = \chi(r_1) \approx r_1 \tag{9}$$

So if we combine equation (8) and (9), we obtain

$$\frac{\Delta t}{a(t_0)} \approx r_1 \tag{10}$$

and plugging this into equation (7) we have

$$z \approx \dot{a}(t_0) r_1 = H_0 d_0 = v|_{t=t_0} \tag{11}$$

where the last expression follows from $\chi \approx r_1$. So this proves that $z \approx v$ for a galaxy that is not far away, which we can interpret in the following way: the cosmological redshift in our cosmic neighbourhood can be seen as a Doppler shift.

Now, let's consider more general expressions that relate the redshift with the evolution of the Hubble's parameter and with the time that passes between emission and observation. From eq. (4) we can get

$$a(t) = a_0 \exp\left[\int_{t_0}^{t} H(t')dt'\right] \tag{12}$$

where $a_0 = a(t_0)$. This can be expanded as a power series around t_0, which leads to

$$a(t) = a_0 \left[1 + H_0(t-t_0) + \frac{1}{2}(H_0^2 + \dot{H}_0)(t-t_0)^2 + \cdots\right] \tag{13}$$

or equivalently

$$a(t) = a_0 \left[1 + H_0(t-t_0) - \frac{H_0^2}{2} q_0 (t-t_0)^2 + \cdots\right] \tag{14}$$

where q_0 is called the *deceleration parameter* defined as:

$$q_0 = -\frac{a_0 \ddot{a}_0}{\dot{a}_0^2} = -\left(1 + \frac{\dot{H}_0}{H_0^2}\right) \tag{15}$$

This parameter (when H_0 is determined) allows us to compute the acceleration or deceleration of the expansion. There has been a lot of effort in the measurement of this parameter in the past three decades, an effort which eventually led to a Nobel prize in Physics in 2011 when it was measured back in 1998 and 1999, and corroborated with further data [1]. The deceleration parameter was found to be negative which implies that $\ddot{a} > 0$, or in words, the Universe expands at an accelerated rate.

This discovery contradicted the natural expectation that matter in the Universe would be decelerating the its expansion due to the gravitational pull (hence the name deceleration parameter).

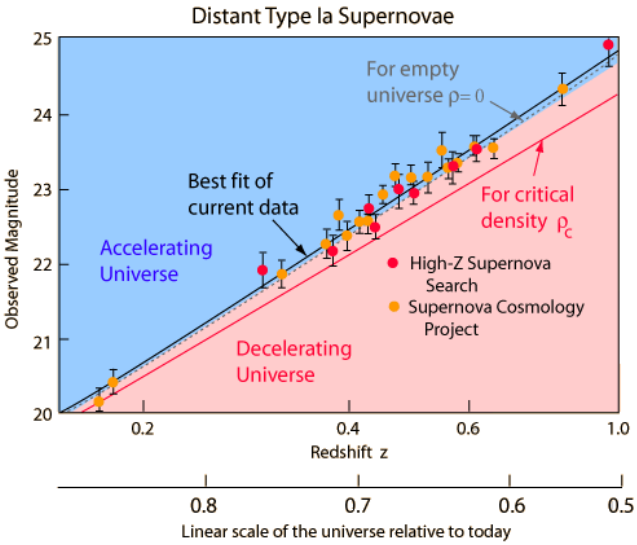

FIG. 1. Type Ia supernovae observations of distant galaxies provided a proof of the Universe accelerated expansion. Here the observed magnitude (related to the intrinsic luminosity of Type Ia supernovae) vs z indicates that the Universe is expanding at an accelerated rate. `http://hyperphysics.phy-astr.gsu.edu/hbase/Astro/univacc.html`

Additional probes of the accelerated expansion of the Universe come from particular features of the cosmic microwave background (CMB) that constraint cosmological parameters. One of them is the large scale plateau of the spectrum of the CMB that suggests an expansion history. The power spectrum of the CMB and the matter power spectrum which is measured from LSS surveys are usually best fit with models that involve a period of late time acceleration. Large surveys of galaxies that observe cosmic shear and its cross-correlation with galaxies provide geometrical probes of dark energy and matter density parameter Ω_m. Moreover, the ISW (Integrated Sachs-Wolfe) effect gives a probe of the expansion through the passing of photons through potential wells of an expanding Universe (although ISW is limited by low S/N ratio) [1].

This result imposes a problem on our understanding of the Universe because this expansion happens to be the dominant component of the energy budget of the Universe now. Different mechanisms to explain the cosmic acceleration have been proposed, most of them involving the existence of a cosmological constant (or vacuum energy), an additional energy component or modifications of gravity [2].

The probes of cosmic acceleration are consistent with a Universe that contains not only matter and radiation, but an additional component that could be the so-called "dark energy", which has an equation of state $w_{\rm DE}$ with negative pressure and that could cause this accelerated expansion. Dark energy is introduced theoretically as a cosmological constant in Einstein's equations and its nature remains unknown. In fact, there have been unsuccessful attempts to relate this dark energy with the vacuum energy from the standard model of particle physics which is based in quantum field theory [3].

So far, the addition of the dark energy is the simplest way to explain the observations of brightness and redshifts for supernovae type Ia (see Figure 1). The nature of the dark energy is perhaps one of the most fundamental problems to be solved in the branch of Cosmology.

III. EFT AS AN UNIFYING FRAMEWORK

In principle we can look for insight into the nature of the accelerated expansion of the Universe through parametrizations of the phenomenology of large scale structure and so we can try to go beyond ΛCDM through parametrized

approaches.

The effective field theory (EFT) of dark energy [4], introduced in the context of inflation and only recently it has been applied to the phenomenon of cosmic acceleration. It is a unifying approach for dark energy and modified gravity models and offers a single parametrization that encloses all single field dark energy and modified gravity models with the advantage that it's fully model independent. The urge for a unifying approach that would parametrize possible deviations from the standard model of cosmology, while still keeping the existing models as special cases and recovering all single-field models in the regime where cosmological perturbation theory can be applied.

Phenomenological functions of large scale structure can be used to parametrize the linear growth of perturbations in a general modification of gravity [5]. The use of viability priors on these phenomenological functions restricts the parameter space so they allow for a model independent approach to GR tests on cosmological scales. These priors are viability conditions based on theoretically motivations and they provide numerical stability.

As said in the introduction, the first assumption to build up the framework starts from the metric. The perturbed FLRW metric in Newtonian gauge (which is characterized by two scalar potentials Ψ and Φ and is a commonly used gauge transformation that allows for identifying "true perturbations") with only scalar perturbations is given by

$$ds^2 = -a^2(\tau)[(1+2\Psi(\tau,\vec{x}))d\tau^2 - (1-2\Phi(\tau,\vec{x}))d\vec{x}^2]\,, \tag{16}$$

Where Φ is the curvature perturbation, Ψ is the newtonian potential. $\Phi+\Psi$ associated to massless particles and thus related to gravitational lensing. In ΛCDM, $\Phi=\Psi$ and $w_{\rm DE}=-1$. Now, by assuming that the metric is coupled to matter fields ψ_m thorough an action $\mathcal{S}_m$. Then the class of Horndeski theories, the EFT action is

$$\begin{aligned}\mathcal{S} = \int d^4x\sqrt{-g}\Big\{ &\frac{m_0^2}{2}\big[1+\Omega(\tau)\big]R + \Lambda(\tau) - c(\tau)a^2\delta g^{00} + \frac{M_2^4(\tau)}{2}\big(a^2\delta g^{00}\big)^2 - \frac{\bar{M}_1^3(\tau)}{2}a^2\delta g^{00}\delta K_\mu^\mu \\ &\frac{\bar{M}_3^2(\tau)}{2}\left[(\delta K_\mu^\mu)^2 - \delta K_\nu^\mu K_\mu^\nu - \frac{a^2}{2}\delta g^{00}\delta\mathcal{R}\right] + \cdots\Big\} + S_m\big[g_{\mu\nu},\chi_m\big]\,,\end{aligned} \tag{17}$$

The functions $\{\Omega(\tau),\Lambda(\tau),c(\tau),M_2^4,\bar{M}_1^3,\bar{M}_3^2\}$ are functions of time which we refer to as the EFT functions. As mentioned in the paper, the functions $\Omega(\tau)$, $\Lambda(\tau)$ and $c(\tau)$ are the only ones that affect the background dynamics. R is the Ricci scalar, δ^{00} is the perturbation of the upper time-time component of the metric, δK_μ^ν and δK_ν^μ perturbations of the extrinsic curvature and its trace, $\delta\mathcal{R}$ the perturbations of the three dimensional Ricci scalar of the constant time hypersurfaces and finally S_m is the action of all matter fields that are coupled to the metric.

The general action is written in the Jordan frame, in which matters follows geodesic of the metric and the gravitational part of the action is modified. Jordan frame is preferred because it is more easily readable from observations and because it is only defined by the coupling to matter. The frame in which the gravitational part of the action is the same as in standard GR, while the matter may be non-minimally coupled to gravity, is called the Einstein frame. This general framework allows us to specify different families of models as we discuss in the next subsection.

A. Chosen models

In order to properly study the effects of all the different EFT operators on the observables, we divide the set of scalar tensor theories in three subsets:

- Generalized Brans Dicke (GBD) is a class of scalar tensor modifications to GR in which the gravitational interaction is mediated by a scalar field as well as the tensor field of general relativity [6]. In this theory, G

(the gravitational constant) is not constant but instead G^{-1} is replaced by a scalar field ϕ which is a function of space and time. The EFT functions which describe this class are those acting on the background operators Λ and Ω. As shown in Figure 2, it is an extension of GR that has a larger parameter space.

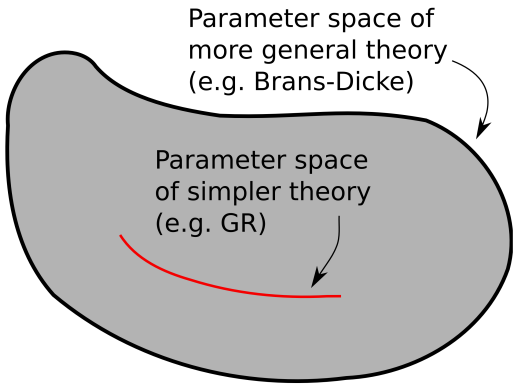

FIG. 2. GBD as a more general theory than general relativity. Image credits: Leo C. Stein, Caltech.

- Horndeski refers to the entire class of single field scalar-field models [7]. In these theories both the scalar and tensor perturbations behave differently from GR [8]. At the level of EFT Horndeski models are described by Λ, Ω, $\bar{M}_1^3$, M_2^4 and $\bar{M}_2^2$. As already stated, this last operator is here set to zero today, in order to be consistent with tensor speed constraint coming from the detection of gravity wave counterpart.

- H_S refers to the subclass of theories in which only the scalar perturbations sector is different from the prediction of GR. In the language of EFT this class is described by Λ, Ω, $\bar{M}_1^3$ and M_2^4.

Name	**EFT functions**
GBD	Ω, Λ
H_S	Ω, Λ, $\bar{M}_1^3$, $\bar{M}_2^4$
Hor	Ω, Λ, $\bar{M}_1^3$, $\bar{M}_2^4$, $\bar{M}_2^2(z=0)=0$

TABLE I. Classes of theories analyzed in this work and corresponding EFT functions.

These subclasses that we use in this work and the relative EFT operators are summarized in Table I. Now, we mention the motivation on the choice of the functions that we sample in this work

B. Choice of phenomenological functions

The functions that come out naturally from this general treatment and that we relate to observables can be used to parametrize departures from ΛCDM. They can be used to parametrize the linear growth of perturbations for modified gravity and dark energy models. They are Σ (sometimes referred as $G_{\rm light}/G$), μ (or $G_{\rm matter}/G$) and the anisotropic stress η. By providing two of these functions we can solve for the evolution of cosmological perturbations since they are related.

In this paper we work with μ and Σ since their link to observables such as WL and ISW for Σ noting that from these two functions we can obtain the anisotropic stress (or gravitational slip) defined as $\eta = \Phi/\Psi$.

Redshift space distortions (usually obtained through extensive spectroscopic galaxy redshifts) will help to measure μ. This function is only relevant in sub-horizon scales and it affects the growth of matter overdensities. and it can be determined from peculiar velocity measurements. Note that in ΛCDM $\mu = 1$.

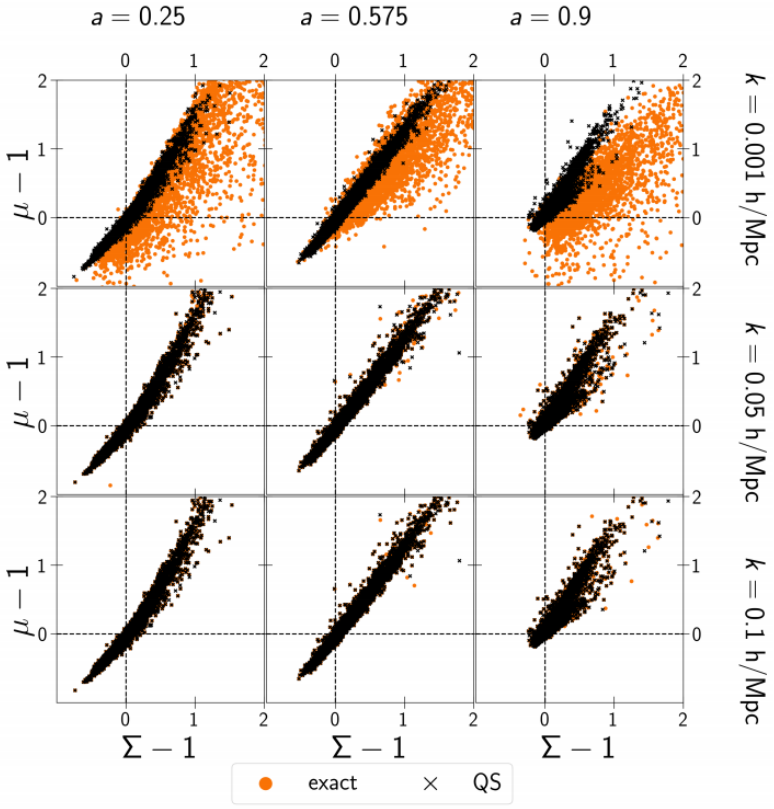

FIG. 3. Correlation between the phenomenology functions $\mu(k, a)$ and $\Sigma(k, a)$ for different cosmic times and scales where the values calculated using the quasi-static approximation (black crosses) and the exact solution (dark orange dots). Figure from [9].

Weak lensing and photometric galaxy counts help constrain Σ which is also referred to as weak lensing function and is directly related to the lensing potential Φ and Ψ. The integrated Sachs-Wolfe (ISW) effect is also sensitive to Σ since it is determined by the time variation of the potential wells that generate the lensing potentials [1].

IV. EXPERIMENTS

There are additional experiments that we don't mention explicitly in the paper but that were part of the process of finding the optimized parameters and ranges for the coefficients in our simulations. Since we need to study how scale dependent our functions are, we decided to run some simulations in which we use different scales $k = \{0.01, 0.085, 0.1\}$. These experiments showed that the scale dependence is irrelevant since the features on the correlation and covariance matrices don't change significantly so and we only needed to make sure that we used a range that allowed for the QSA and that assured that the linear theory was still valid. In [9] they sample μ and Σ in the ranges a=0.25,0.575,0.9 and k=0.001, 0.005, 0.1 as shown in Figure 3 so as mentioned in the paper, the QSA works quite well for our chosen scale.

Additionally, we wanted to check the consistency of our results with the work conducted in [10] and we see that we successfully reproduce the plots of the paper of $w_{\rm DE}(z)$ (with and without the mild observational constraint of SN), noting that we impose a hard bound on the speed of gravitational waves today and that we use a specific value of k and a different redshift range (which is irrelevant for the overall result):

Also, we check how the acceptance ratio is affected with the variation of the range in the coefficients finding no difference in the resulting features. As mentioned in the paper, we consider models that are close to ΛCDM in the

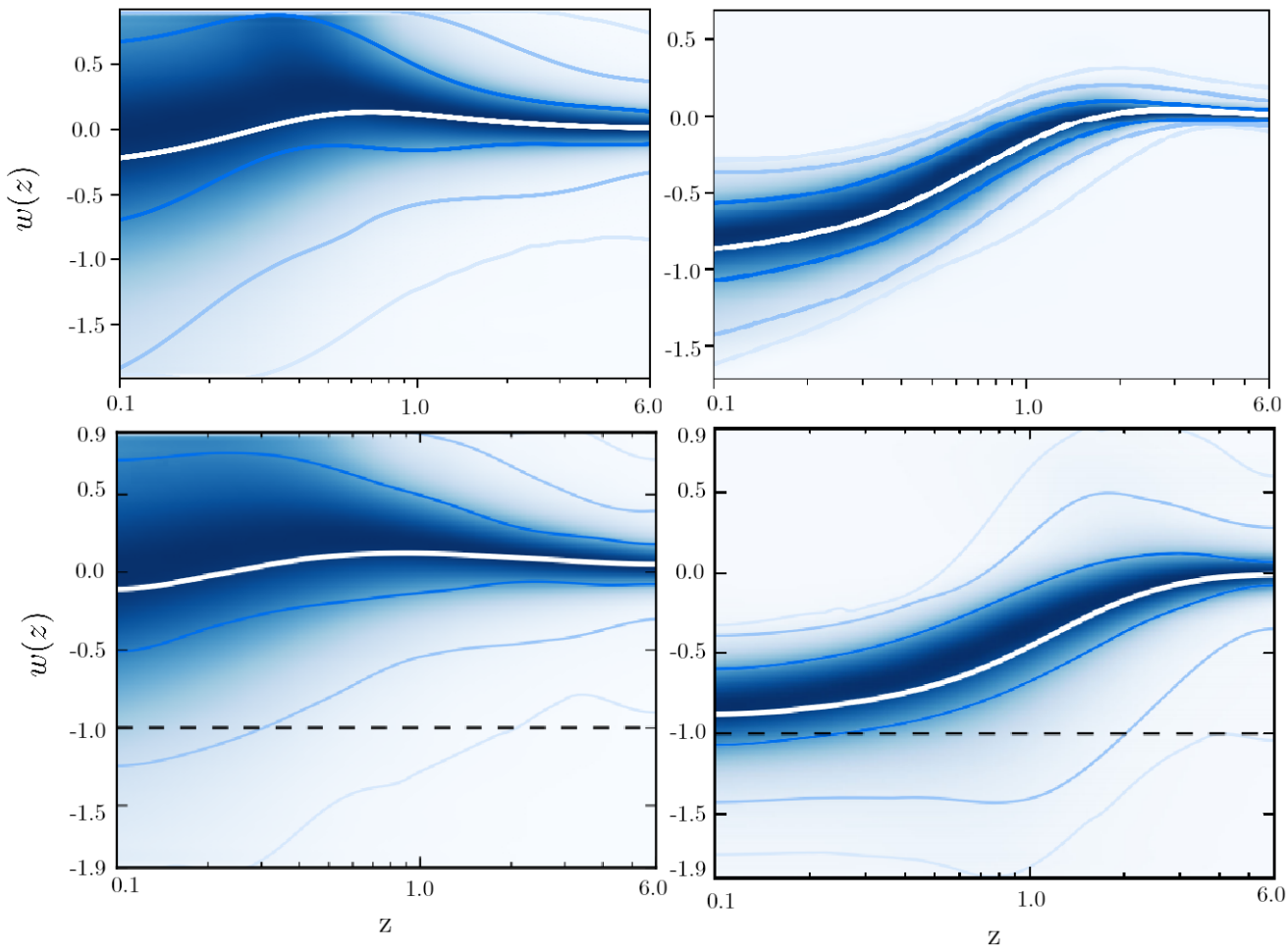

FIG. 4. Comparison between our results and the ones produced in for $w_{\rm DE}$. The plots on the left are produced with all the observational constraints, and the ones at the right are produced without those constraints. One of the small differences in our data (top row) compared to the data from [10] (bottom) is the hard bound on $\alpha_T(z=0)=0$ based on the detection of GW170817 and GRB170817A [11][12][13].

past and in the present, namely thawing ($a_0=0$) or freezing ($a_0=1$).

An additional experiment in our work is the projection of these samples to a certain known parametrization. In our case, we used the CPL (Chevallier-Polaski-Linder) parametrization: $w_{\rm DE}=w_0+w_a(1-a)$ where

$$w_a=-\frac{dw_{DE}}{da}\bigg|_{a=1} \tag{18}$$

As of now, these projections haven't been completed and thus it's not useful to include them as part of the work but will certainly be part of future research given the potential of the data.

Features on the correlations are better read off the covariance matrices (or dispersion matrices), which show the covariance between the functions at different values of scale factor. Using Eq. (12) we compute many correlation matrices for all the cases searching for prominent features as displayed in figure 5. One particular procedure that took some time was the different colour scales and colour ranges that allowed us to compare between the different models. This is because each model produces different types of outliers that can drag the colour bars differently and thus hide many of the important features.

Regarding this, we also need to apply some filters on the final samples for very few outliers that wouldn't damage

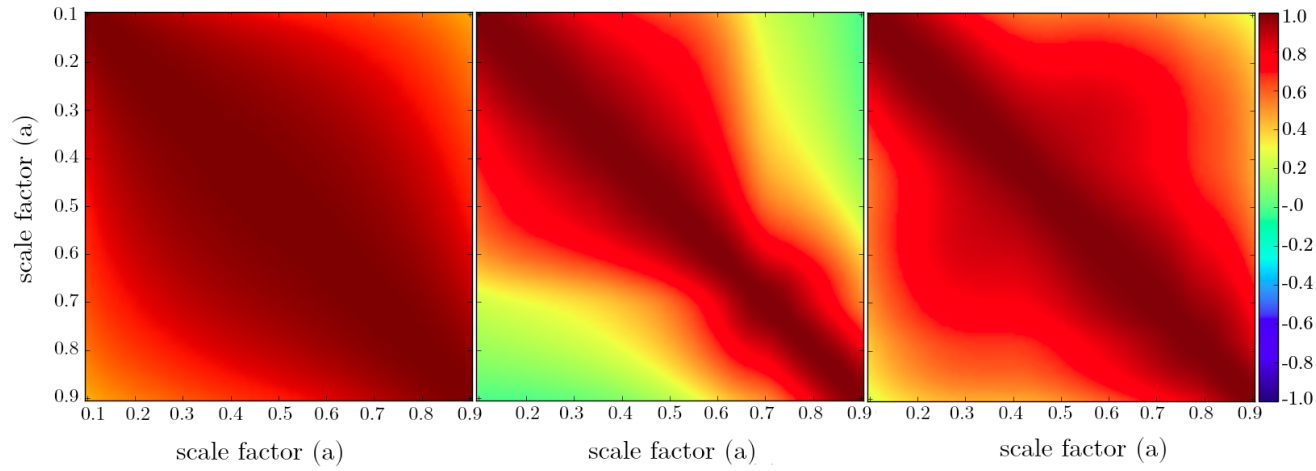

FIG. 5. Correlation matrices for μ for runs with stability and observational constraints in the freezing case (a_0 =1). From left to right: GBD, H_S and Horndeski

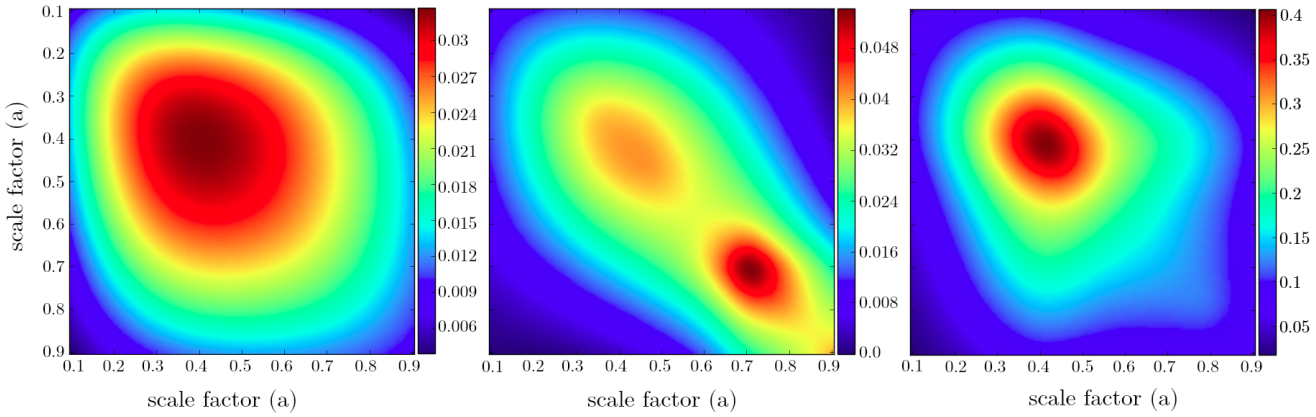

FIG. 6. Covariance matrices for μ for runs with stability and observational constraints in the freezing case (a_0 =1). From left to right: GBD, H_S and Horndeski. Colour bars have very different ranges so it's necessary to use the right range for visualization.

the statistics of the correlation length calculations but would bring peaks in the covariance and correlation matrices that make the important features obscure.

Using Eq. (11) we calculate the covariance matrices that complement correlation matrices and show features more clearly. Figure 6 shows the covariance matrices for our three chosen models where the large difference in the colour bar can be seen.

By calculating the autocorrelation (defined as the variance) of the models we can see more clearly the scale of the bumps on the covariance and at what scale factor values these correlations change.

Best fit correlation

	μ	Σ	$w_{\rm DE}$
GBD	$\exp\left[-\left(\lvert\delta a\rvert/0.94\right)^{2.85}\right]$	$\exp\left[-\left(\lvert\delta a\rvert/0.82\right)^{2.38}\right]$	$\left(1+\left(\lvert\delta\ln a\rvert/0.29\right)^{3}\right)^{-1}$
HS	$\left(1+\left(\lvert\delta a\rvert/0.28\right)^{2.41}\right)^{-1}$	$\exp\left[-\left(\lvert\delta a\rvert/0.42\right)^{1.5}\right]$	$\left(1+\left(\lvert\delta\ln a\rvert/0.3\right)^{2.9}\right)^{-1}$
Hor	$\left(1+\left(\lvert\delta a\rvert/0.3\right)^{1.9}\right)^{-1}$	$\left(1+\left(\lvert\delta a\rvert/0.3\right)^{1.9}\right)^{-1}$	$\left(1+\left(\lvert\delta\ln a\rvert/0.3\right)^{2.9}\right)^{-1}$

TABLE II. Best fit correlation lengths computed for our three chosen models for μ, Σ and $w_{\rm DE}$ from equations (13) and (14) from the main paper. These found values are a first step to a non-parametric reconstruction of the phenomenological functions.

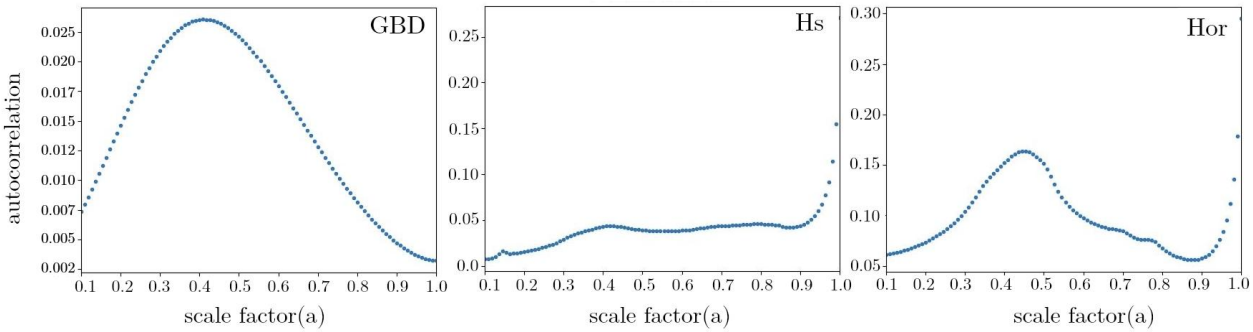

FIG. 7. Sigma autocorrelation (variance) for the runs with the observational constraints except for SN. The peaks in these plots are the colour peaks of figure 6.

The bumps in Figure 6 are probably due to some of the imposed constraints so it was worth it to make different experiments with the variations of these constraints, especially those in Ω. What we found from running simulations where none of the constraints were imposed is the bump clearly disappears for GBD, but it stays for Horndeski. That's why we assume the bump must be driven by α_T and therefore we made runs without any constraints whatsoever so we could check how α_T is naturally sampled as discussed in the paper.

Using equations (13) and (14) we find the best fit values for the correlations given the additional features and broad behaviour that we found in the correlation matrices for μ and Σ. Figure 8 shows the

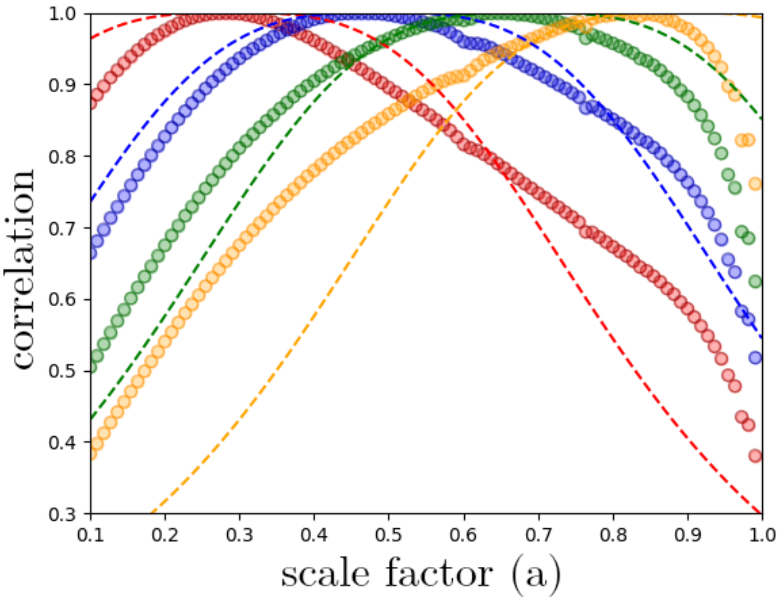

FIG. 8. Best fit for the correlation profile at different values of scale factor. Filled round markers show for the data and dashed line for the analytical correlation. Since the results of these fits are not very satisfactory we will explore different parametrizations for the coming work.

As explained in the summary section of the main paper, these results constitute the first steps on the construction of non-parametric analytical functions of μ and Σ and will give some insight into what future surveys should focus on. Additionally it is one of many works in the direction of finding a successful theory of gravity that will for sure change our understanding of the Universe.

ACKNOWLEDGMENTS

I would like to thank my supervisor Alessandra Silvestri for her kind support and clear explanations in many of these topics completely new for me. She encouraged me to not only do my research project but also to work on my first publication. Her optimistic attitude and compromise for work is a motivation to keep on working on science. Many thanks to Simone Peirone who was always willing to help me with any question especially with the computational part. I would like to extend my gratitude to Marco Raveri, Levon Pogosian and Kazuya Koyama as collaborators on the paper and their always kind support with any of my questions.

Finally, I would like to mention that the support of my family, friends and girlfriend were a big part of this process so I would like to extend my gratitude to them as well.

---

[1] A. Silvestri and M. Trodden, Rept. Prog. Phys. **72**, 096901 (2009), arXiv:0904.0024 [astro-ph.CO].
[2] B. Jain and P. Zhang, Phys. Rev. **D78**, 063503 (2008), arXiv:0709.2375 [astro-ph].
[3] P. Horava, Phys. Rev. **D79**, 084008 (2009), arXiv:0901.3775 [hep-th].
[4] F. Piazza and F. Vernizzi, Class. Quant. Grav. **30**, 214007 (2013), arXiv:1307.4350 [hep-th].
[5] L. Pogosian and A. Silvestri, Phys. Rev. **D94**, 104014 (2016), arXiv:1606.05339 [astro-ph.CO].
[6] C. Brans and R. H. Dicke, Phys. Rev. **124**, 925 (1961).
[7] G. W. Horndeski, Int. J. Theor. Phys. **10**, 363 (1974).
[8] R. Kase and S. Tsujikawa, Int. J. Mod. Phys. **D23**, 1443008 (2015), arXiv:1409.1984 [hep-th].
[9] S. Peirone, K. Koyama, L. Pogosian, M. Raveri, and A. Silvestri, Phys. Rev. **D97**, 043519 (2018), arXiv:1712.00444 [astro-ph.CO].
[10] M. Raveri, P. Bull, A. Silvestri, and L. Pogosian, Phys. Rev. **D96**, 083509 (2017), arXiv:1703.05297 [astro-ph.CO].
[11] D. Blas, M. M. Ivanov, I. Sawicki, and S. Sibiryakov, (2016), arXiv:1602.04188 [gr-qc].
[12] B. P. Abbott *et al.* (Virgo, LIGO Scientific), Phys. Rev. Lett. **116**, 061102 (2016), arXiv:1602.03837 [gr-qc].
[13] B. P. Abbott *et al.* (Virgo, Fermi-GBM, INTEGRAL, LIGO Scientific), Astrophys. J. **848**, L13 (2017), arXiv:1710.05834 [astro-ph.HE].